Ai, Q., & Weaver, P. M. (2017). A Multi-stable Spanwise Twist Morphing Trailing Edge. In 25th AIAA/AHS Adaptive Structures Conference. [AIAA 2017-0055] American Institute of Aeronautics and Astronautics Inc, AIAA. DOI: 10.2514/6.2017-0055

Peer reviewed version

A Multi-stable Spanwise Twist Morphing Trailing Edge

Qing Ai*, Paul M.Weaver†
University of Bristol, Bristol, United Kingdom, BS8 1TR

A spanwise morphing trailing edge design utilizing structural multistability with minimised actuation requirements is introduced in this paper. The proposed morphing device consists of composite laminate spars and ribs assembled in a grid pattern. The composite laminate spar strips are manufactured in a stress free state with a predefined curvature and are prestressed by flattening before assembly. In this way, initial strain energy is stored in structural components that can later be released during structural deformations. With an analytical model, design parameters including laminate layups of spars and the initial curvature in spar strips are investigated. Results show that by selectively changing the structural design, the stable equilibria configuration of the morphing device can be set over a wide range of twist angles. Particularly, a zero torsional stiffness spanwise morphing trailing edge design has been observed. Finite element method results are provided to verify the analytical model and good correlation is found. The spanwise trailing edge deformed shape of the novel device features a desirable torsion behavior, providing structural conformality and a constant torsion angle variation along the span. Comparison with a flap transition design from the literature indicates that further optimization of the profile can lead to improved aerodynamic performance.

Nomenclature

b	=	trailing edge chord length
c	=	aerofoil chord length
E	=	Young's modulus
G	=	shear modulus
M	=	twist moment
GJ	=	torsional stiffness
l	=	spar rib length
L	=	trailing edge span length
Π	=	strain energy
D^*	=	laminate reduced flexural stiffness matrix
R	=	distance between spar and the twist axis
ρ	=	radius of curvature of the pre-bend spar strips
δ	=	ratio of l to ρ, $\frac{l}{\rho}$
β	=	laminate ply angle
ν	=	Poisson's ratio
κ	=	curvature

*PhD Student, Advanced Composites Centre for Innovation and Science (ACCIS), University of Bristol. qing.ai@bristol.ac.uk
†Professor in Lightweight Structures, Advanced Composites Centre for Innovation and Science (ACCIS), University of Bristol, Paul.Weaver@bristol.ac.uk

I. Introduction

Aviation industries are driven by ongoing economic and environmental considerations for aeroplanes of high efficiency and low gas and noise emission [1]. Of particular importance is to maintain aeroplane performance based on varying flight regimes. As such, shape changing structures that have excellent performance characteristics, low system complexity and potential light-weight have received growing interest from the engineering community. These intelligently responsive structures are increasingly known as morphing structures and have been considered as promising candidates for the next generation of high-lift systems for aeroplane wings. [2–4]

Conventional multi-element aeroplane wings including ailerons and flaps use discrete rigid structural parts that are articulated around hinges and linkages to provide required geometrical changes for flow control purposes. Such a design philosophy leads to a heavy system and a high mechanism complexity. On the contrary, morphing structures enable wing surface geometrical changes to happen through conformal structural deformations including bending and twisting, reducing system complexity and weight [2, 3, 5–8]. Furthermore, the intrinsic continuous geometrical changes and smooth structural surfaces in morphing structures significantly reduce drag forces and noise emission due to structural discontinuities [5].

Aerofoil morphing concepts are primarily classified into two main categories: in-plane morphing and out-of-plane morphing with chordwise, spanwise profile change and twist being three different ways for enabling out-of-plane morphing structures [3]. Chordwise morphing structures have received significant interest in recent decades. Campanile *et al.* [9] developed a chordwise morphing aerofoil concept, the Belt-Rib, consisting of a closed belt and spokes. Experimental studies have successfully confirmed the feasibility of the concept for aerofoil flow control purposes. Results showed that tailoring of the structural stiffness of the Belt-Rib can lead to significant aerodynamic and aeroelastic amplification effects, minimising the external actuation requirement. Furthermore, variable stiffness materials have also been studied for application in morphing structures due to efficiency and performance considerations [10, 11]. Ai *et al.* [11] introduced material stiffness variations into a chordwise morphing trailing edge design that facilitated tailoring of morphing profiles of the deformed trailing edge. Studies of aerofoils fitted with such morphing trailing edges showed that the aerofoil performance envelope including lift and drag coefficients and noise emission can be effectively extended [12, 13]. However, even though a continuous aerofoil camber change is achieved with the morphing trailing edge concepts, spanwise end gaps remain between adjacent trailing edge flaps that could lead to increased noise emission and drags. To address this issue, different flap transitions linking flaps in a spanwise fashion have been proposed in recent decades [14–17]. Woods *et al.* [17] proposed an elastically lofted transition control surface for wings which covers the gaps between spanwise ends of adjacent control surfaces. The proposed morphing transition control surface constitutes a series of stacked ribs with skewed corrugations along the wing span exploiting material and geometric compliance with bend-twist coupling. Desired spanwise nominal deformation shapes can be obtained with carefully selected corrugated skewed rib angles.

Similar to spanwise flap transitions, wing twisting also provides continuous spanwise profile change and several concepts have been proposed and studied [3, 18, 19]. Lachenal *et al.* [18] proposed a zero torsional stiffness (ZTS) twist morphing blade structure which consisted of pre-stressed flanges and a warping skin as actuation method. A proof-of-concept demonstrator was manufactured and investigated with an analytical model, finite element method (FEM) and also experiments. Results showed that by tailoring the prestress in the flanges, a twist morphing blade with zero torsional stiffness about its rotation axis can be obtained. However, discrepancies between the analytical results and experimental measurements were observed for large twist angles, owing to the simplicity of the analytical model. Following this study, Daynes *et al.* [19] developed a zero torsional stiffness morphing aerofoil which is made of precurved carbon fibre reinforced plastic (CFRP) laminate spar strips and CFRP ribs. The multistable twisting structure was studied with an analytical model and then validated against FEM and experimental results. Good agreement was found between results from the analytical model and that from FEM. The study showed that the combination of geometry nonlinearity, material properties and pre-stress effects in the morphing structure can lead to a significant reduction in actuation energy requirements and a zero torsional stiffness design case was also observed.

In this paper, a novel spanwise twist morphing trailing edge (SMTE) concept is developed using prestressed composite laminate spar strips. Prestress effects in structures have been used previously to adaptively change the structural stiffness [20] and the proposed SMTE concept extends on previous research work by Lachenal [18] and Daynes [19]. It is observed that in recent morphing wings [18, 19], geometrical changes were achieved by twisting the whole wing about an axis, which leads to coupled deformation in both the leading edge and trailing edge parts. The developed SMTE herein can be attached to a wing leading edge part that decouples the deformation in the trailing edge and leading edge parts. This paper is organized as follows: the SMTE design is introduced firstly with geometric parameters given and then a simple analytical model of the SMTE structure is described in detail; preliminary investigations on effects of changing laminate ply angles and initial curvatures are then discussed to study the stability of the SMTE; finite element method is used to validate a zero torsional stiffness SMTE design case and the paper finishes by discussing

results and giving conclusions.

II. The spanwise morphing trailing edge concept

Over recent decades, several aeroplane wing flap transition devices have been proposed [14–16], most of which use mechanical systems to provide the desired spanwise trailing edge deformed shape. However, one significant challenge remaining is the actuation requirement for such devices. Not only do they have complex driving mechanisms, but also require large amount of actuation energy. To address this issue, a multistable SMTE concept is proposed, which is able to provide a spanwise trailing edge deformed shape featuring twist/torsion structural behavior with minimum actuation force requirements.

A SMTE device can be used as a single function unit for spanwise wing geometrical changes and can also serve as a smooth transition between different control surfaces. Using such concepts, the drag force and wing noise emission can be reduced by removing flow vortices around the flap ends from the pressure side to the suction side [5]. In this section, a SMTE design consisting of composite laminate spars and ribs is introduced and an analytical model is developed to describe the mechanical behavior of the structure. Ideally, an aeroelastic approach coupling fluid and structural analyses is desirable in the morphing structure design and a solution that suits a wide range of flow conditions is realistic and viable. However, in this SMTE concept, the flow field around the trailing edge depends greatly on the flow velocity, angles of attack and the deformed shape (both spanwise and chordwise) of the morphing trailing edge. Accurate aerodynamic pressure and force calculations in this case require computationally expensive three-dimensional computational fluid dynamic simulations and the coupled fluid-structure interaction can significantly complicate the design process. Thus, the current research only focuses on the concept development and effects of aerodynamic forces are not considered in this preliminary design study.

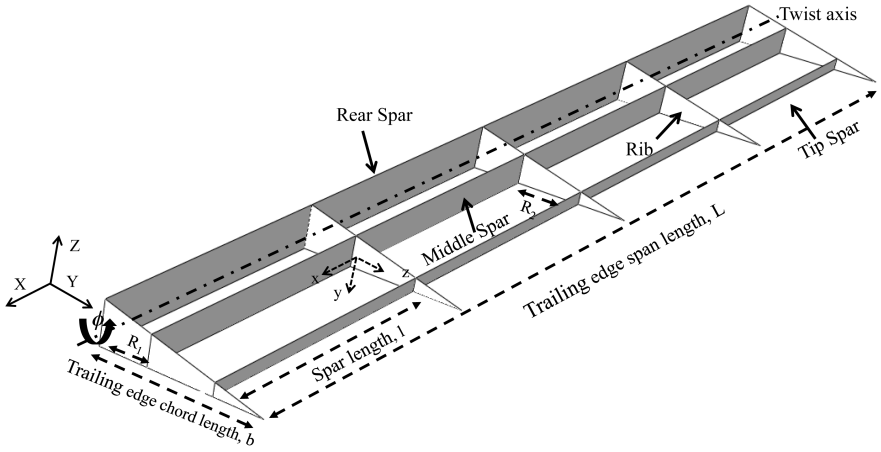

Figure 1. Schematic of the spanwise morphing trailing edge design

A. SMTE design

The proposed SMTE concept consists of two main components: ribs along chord and spars in the span direction, which are assembled in a grid pattern. A NACA 0012 aerofoil is chosen in this study. The wing has a chord of c = 500 mm and a trailing edge length of b = 100 mm (b/c =20%). The span length, L, is 600 *mm* and five ribs are evenly arranged along the wing span. Three rows of spar strips are used: the rear, middle and tip spars, as shown in Fig. 1 and the spar strip length, l is 150 *mm*. The distances from rear spar to middle spar, R_1 and from the middle spar to the tip spar, R_2, are 30 *mm* and 40 *mm*, respectively. This paper focuses on describing a generic concept of a twist morphing trailing edge instead of developing a product for any specific application and as such, geometrical parameters used are for general purposes and not optimized. All the rib and spar strips are made of composite laminates using Hexcel 8552/IM7 CFRP prepreg [21] with mechanical properties given in Table. 1. All ribs have the same laminate layup of $[0_4]$ with 0° along chord and the spar ribs ply angle β is considered as a design parameter for a layup of $[\beta_8]$ with 0° along span. It is worth noting that prestress effects are only introduced into the the middle and tip spar strips (see Fig. 1) with an initially manufactured curvature before assembly.

The twist axis is positioned at the centroid of the rear spar and does not coincide with the shear centre of the

Table 1. Material properties of prepreg material [21]

Material	E_{11} (GPa)	E_{22}(GPa)	G_{12}(GPa)	$\nu_{12}(--)$	$\nu_{21}(--)$	Thickness (mm)
8552/IM7	135	9.5	5	0.3	0.021	0.125

structure. The offset between the selected twist axis and the structural shear centre leads to a spanwise bending deformation and such effects can be minimised by optimizing the positions of the middle and tip spar, *i.e.* R_1 and R_2, which is not considered in detail in this paper. Rear spar strips are manufactured flat without an initial curvature while the middle and tip spar laminate strips are manufactured in a stress free state with an initial curvature $\kappa_{x,initial}$ along its local x axis (see the coordinate system in dashed line Fig. 1). The grid structure is then built in a heightened energy state and the pre-stored energy in the flattened spar strips can be released during the twist deformation to reduce the work done by the actuation force.

B. Analytical model

1. *Strain energy* Π

The internal grid structure of the SMTE is inspired by the morphing aerofoil device by Daynes *et al.* [19]: two prestressed spars are held at a distance R_i from the twist axis at the centroid of the rear spar and are subject to twist deformation about the twist axis under applied actuation moment. In this paper, the inextensible model developed by Daynes *et al.* [19] is adopted. Key assumptions are: (1) the laminate strip deformation is inextensible and (2) the curvature is uniform across the mid-surface of the strips. When the SMTE is subject to a twist angle ϕ at the spanwise end, as shown in Fig. 1, the curvature change $\triangle\kappa$ of a spar strip with respect to its local coordinate (see coordinate system in dashed line in Fig. 1) is expressed as follows [19]:

$$\triangle\kappa = \begin{bmatrix} \triangle\kappa_x \\ \triangle\kappa_y \\ \triangle\kappa_{xy} \end{bmatrix} = \begin{bmatrix} \frac{R_i \cdot \phi^2}{2L^2} - \kappa_{x,initial} \\ 0 \\ 2\frac{\phi}{L} \end{bmatrix}, \tag{1}$$

where R_1 denotes the distance between the rear spar and middle spar, R_2 refers to the distance between the middle spar and tip spar, L is the SMTE span length, $\kappa_{x,initial}$ is the initial bend curvature in the middle and tip spar strips, defined as $\kappa_{x,initial} = 1/\rho$ with ρ denoting the initial radius of curvature in the pre-bend strips. An assumption is made that the transverse curvature is negligible, which is valid for slender strips where the strain energy from longitudinal curvature and twist are dominant. However, a thorough study has been carried out by Lachenal *et al.* [22] to investigate effects of the transverse curvature on the stability of helix structures. It was found that membrane stretching occurs when the transverse curvature is considered and a two-dimensional, extensional model can provide explicit insight into the mechanical behavior. In the following sections, investigations are carried out with the current analytical formulations owing to its combined simplicity and sufficient level of accuracy.

The structural strain energy Π is expressed as: [23]

$$\Pi = \frac{1}{2}\sum_{i=1}^{N} l_i H_i \triangle\kappa_i^T D_i^* \kappa_i, \tag{2}$$

where N represents the total number of spar strips in the structure, l_i and H_i denotes the length and width of the i^{th} strip respectively, $\triangle\kappa_i^T$ refers to the transpose of the curvature change tensor $\triangle\kappa_i$, D_i^* is the reduced flexural stiffness matrix of the composite laminate spar strips and is defined as, $D^* = D - BA^{-1}B$, where A, B and D are the in-plane, coupling and flexural stiffness matrices in classic laminate theory [24].

Combining Eqs. 1 and 2, the strain energy is calculated as:

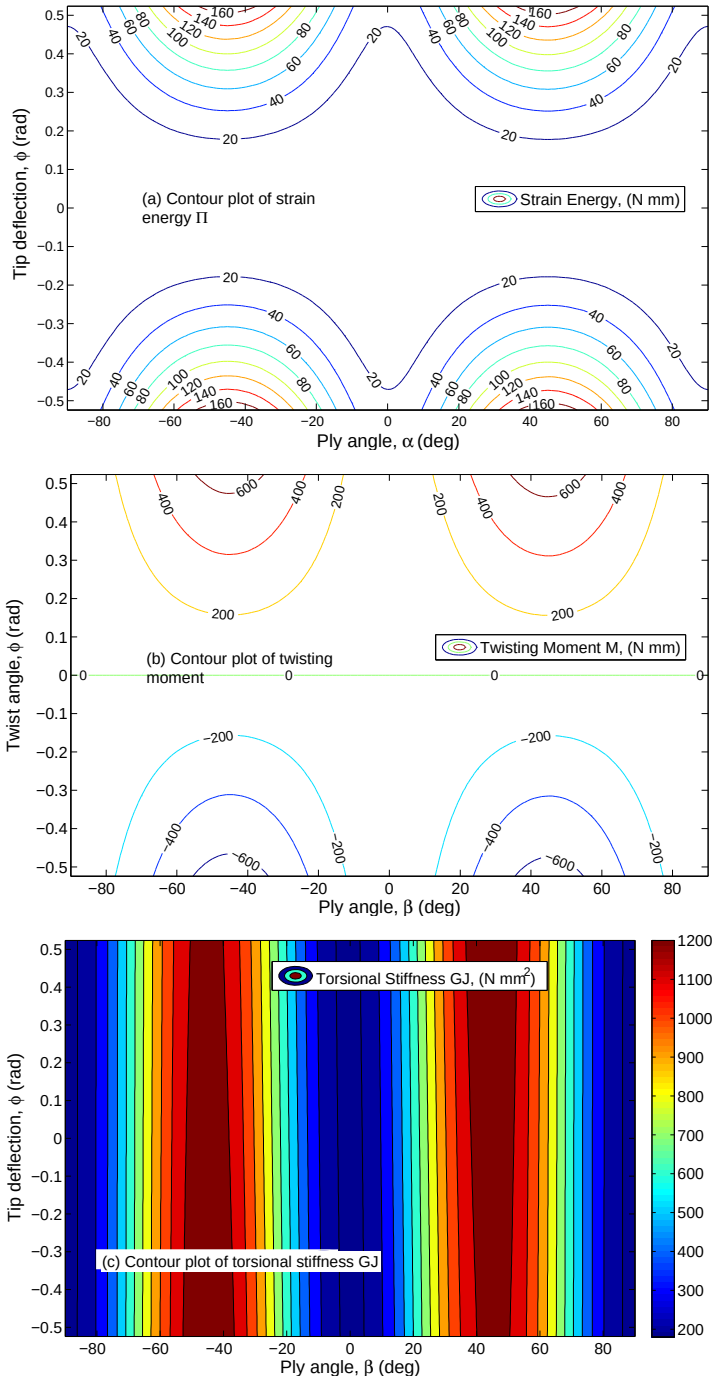

Figure 2. Effects of the ply angle β and twist angle ϕ for $\delta = 0$ on the structural behaviors: (a) contour plot of strain energy Π, (b) twisting moment M and (c) torsional stiffness GJ.

$$
\begin{aligned}
\Pi &= \frac{1}{2}\sum_{i=1}^{N} l_i H_i \triangle\kappa_i^T D_i^* \kappa_i \\
&= \frac{1}{2}\sum_{i=1}^{N} l_i H_i \{D_{11,i}^*(\triangle\kappa_{x,i})^2 + 2D_{16,i}^*(\triangle\kappa_{x,i}\triangle\kappa_{xy,i}) + D_{66,i}^*(\triangle\kappa_{xy,i})^2\} \\
&= \frac{1}{2}\sum_{i=1}^{N} l_i H_i \{D_{11,i}^*(\frac{R_i\cdot\phi^2}{2L^2} - \kappa_{x,initial})^2 + 2D_{16,i}^*(\frac{R_i\cdot\phi^2}{2L^2} - \kappa_{x,initial})(2\frac{\phi}{L}) \\
&\quad + D_{66,i}^*(2\frac{\phi}{L})^2\},
\end{aligned}
\tag{3}
$$

where $D^*_{11,i}$ $D^*_{16,i}$ and $D^*_{66,i}$ are the stiffness components of the reduced flexural stiffness matrix of the i^{th} laminate spar strip. As the spar laminate strips are constrained from warping at both ends, the torsional stiffness has been effectively increased and the modified stiffness is expressed as: [19]

$$D^*_{66,new} = \frac{D^*_{66}}{1 - \frac{H_i}{12 l_i}\sqrt{\frac{10E_{11}}{G_{12}}}}, \tag{4}$$

where E_{11} and G_{12} are the longitudinal Young's modulus and in-plane shear modulus and given in Table. 1.

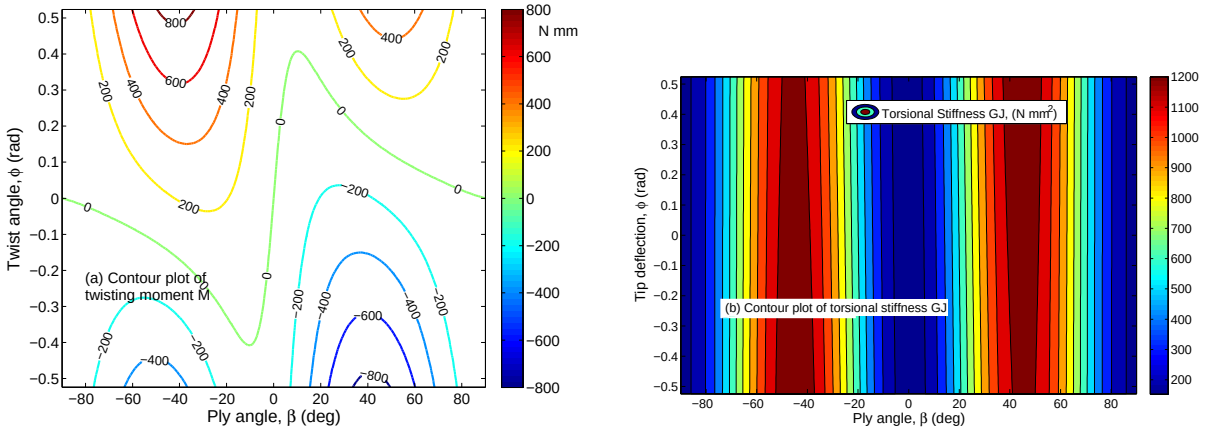

Figure 3. Effects of the ply angle β and twist angle ϕ for $\delta = 0.2$ on the structural behaviors: (a) twisting moment M and (b) torsional stiffness GJ.

2. *Energy stable equilibria*

The stable equilibria of the SMTE can be found by seeking the minimum strain energy state in terms of design parameters, *i.e.* the laminate ply angle β for all the spar strips, the initial pre-bend curvature $\kappa_{initial}$ in the middle and tip spars and the twist angle ϕ [19, 25]. The stable equilibrium configurations are determined when the first derivative of the strain energy Π is zero and the second derivative of Π is greater than zero. The twisting moment (M) and torsional stiffness (GJ) of the structural stability criteria are then expressed as:

$$\begin{aligned} M &= \frac{\partial \Pi}{\partial \phi} = 0, \\ GJ &= \frac{\partial M}{\partial \phi} = \frac{\partial^2 \Pi}{\partial \phi^2} > 0. \end{aligned} \tag{5}$$

III. Strain energy tailoring

Using current analytical formulations of the strain energy and the stable equilibria conditions developed in the previous section, Eq.3 and 5, a preliminary optimization study is carried out to investigate the stability of the SMTE. Design parameters considered in this study are the initial pre-bend radius of curvature ρ of the middle and tip spar strips, the spar laminate strip stiffness matrix D^* and the twist angle ϕ applied to the SMTE. In order to simplify the analysis, only symmetric laminates with the same orientation angle β (see Fig. 1) with constant thickness of 1 *mm* are considered for all spar strips, *i.e.* a layup of $[\beta_8]$. The ply angle varies from $-90°$ to $90°$ to cover the whole ply angle range. The twist angle ϕ is selected to change from $-30°$ to $30°$, which provides a large deformation capability for the SMTE. A parameter δ, is defined as the ratio of the spar length l to the initial pre-bend radius of curvature ρ, *i.e.* $\delta = l/\rho$. After a parametric sensitivity study, a range of [0,1.5] is selected for δ. Effects of the ply angle β and δ on the stability of SMTE are studied and discussed in detail in the following sections.

A. Ply angles

Figure. 2 presents the contour plot of strain energy Π, twisting moment M and torsional stiffness GJ of the SMTE as a function of the ply angle β of the laminate spar strips for a zero initial curvature in the middle and tip spars (see Fig. 1). Without the prestress effects in the spars, the strain energy Π increases with the twist angle ϕ for all ply angles and peaks are found at ply angles $\beta = \pm 45^\circ$ and twist angle $\phi = \pm 30^\circ$. A unique stable equilibrium is found at $\phi = 0^\circ$ where the condition $M(\phi = 0^\circ) = {}^{\partial\Pi}/_{\partial\phi} = 0$ (Fig. 2b) and $GJ(\phi = 0^\circ) = {}^{\partial^2\Pi}/_{\partial\phi^2} > 0$ (Fig. 2c) are satisfied. As expected, a ply angle of $\beta = \pm 45^\circ$ provides the highest torsional stiffness and hence requires the greatest twist moment. Without any pre-stored strain energy, the neutral position of the SMTE is only possible with $\phi = 0^\circ$, which corresponds to a minimum strain energy state for the SMTE.

The twist moments and torsional stiffness of the SMTE for non-zero initial curvature $\kappa_{x,initial}$ ($\delta = 0.2$, 0.6 and 1.3) are shown in Figs. 3 to 5, respectively. As the SMTE is now assembled in a heightened energy state, the stable equilibria configurations become dependent on the ply angle β and δ. The lines where the twisting moment is zero ($M = 0$) in Figs. 3a and 4a indicate the stable equilibria configurations of the SMTE, corresponding to positive stiffness GJ in Figs. 3b and 4b, respectively. In Fig. 3a, for $\delta = 0.2$, the stable configuration varies from $\phi = -0.4$ *rad* with a ply angle of $\beta \approx -10^\circ$ to $\phi = 0.4$ *rad* with a ply angle of $\beta \approx 10^\circ$. Interestingly, one stable configuration corresponds to two different ply angles. As the initially stored energy further increases to $\delta = 0.6$, the stable twist angle of the SMTE further extends to ± 0.524 *rad* ($\pm 30^\circ$), as shown in Fig. 4a. Similarly, every stable equilibrium corresponds to two ply angles, one of which is in a narrow range about $\beta = 0^\circ$. It is worth noting that the stable neutral position of the SMTE proposed can now be predefined over a wide range of twist angles ϕ (in this case, $\phi_{stable} = \pm 0.524$ is achievable) by selectively designing the ply angle and the initial curvature in the middle and tip spar laminates.

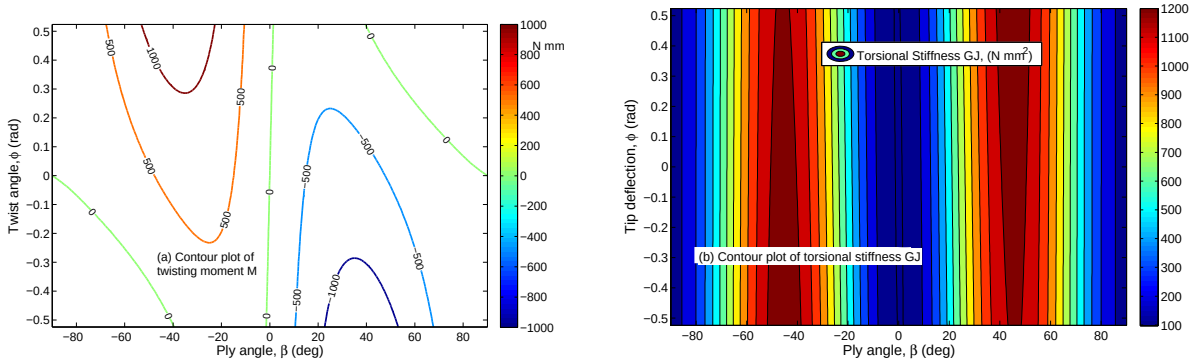

Figure 4. Effects of the ply angle β and twist angle ϕ for $\delta = 0.6$ on the structural behaviors: (a) twisting moment M and (b) torsional stiffness GJ.

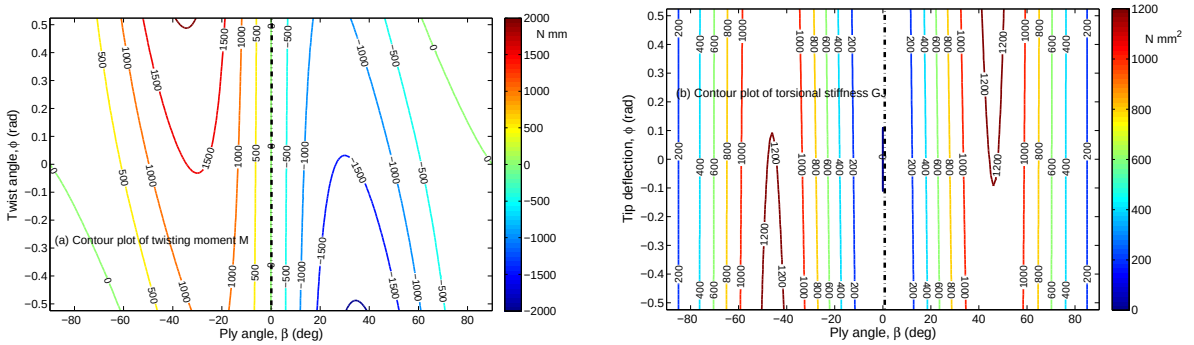

Figure 5. Effects of the ply angle β and twist angle ϕ for $\delta = 1.3$ on the structural behaviors: (a) twisting moment M and (b) torsional stiffness GJ.

Particular attention is paid to a design case with $\delta = 1.3$ where a zero torsional stiffness SMTE is observed. As shown in Figs. 5a and 5b, the dotted line for a ply of angle $\beta = 0^\circ$ shows that for all twist angles from $\phi = -0.524$ to $\phi = 0.524$, the twisting moment M and torsional stiffness GJ remain unchanged at a value of zero and the required

actuation twist moment hence becomes zero. The ZTS SMTE observed herein is discussed in detail in Section 7.6.

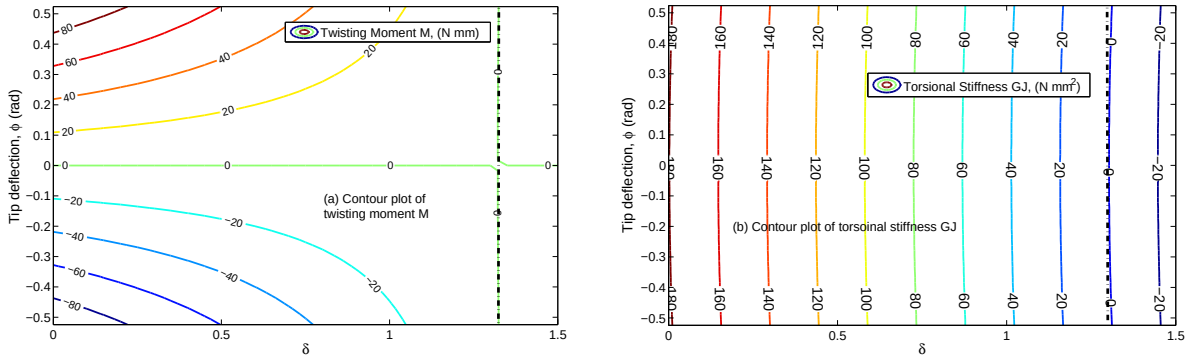

Figure 6. Effects of δ and twist angle ϕ for spar strips with a ply angle of $\beta = 0°$ on: (a) twisting moment M and (b) torsional stiffness GJ.

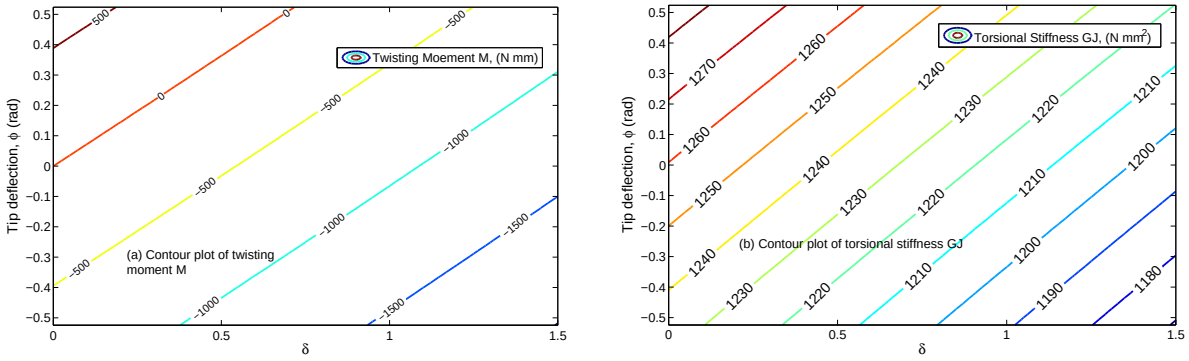

Figure 7. Effects of δ and twist angle ϕ for spar strips with a ply angle of $\beta = 45°$ on: (a) twisting moment M and (b) torsional stiffness GJ.

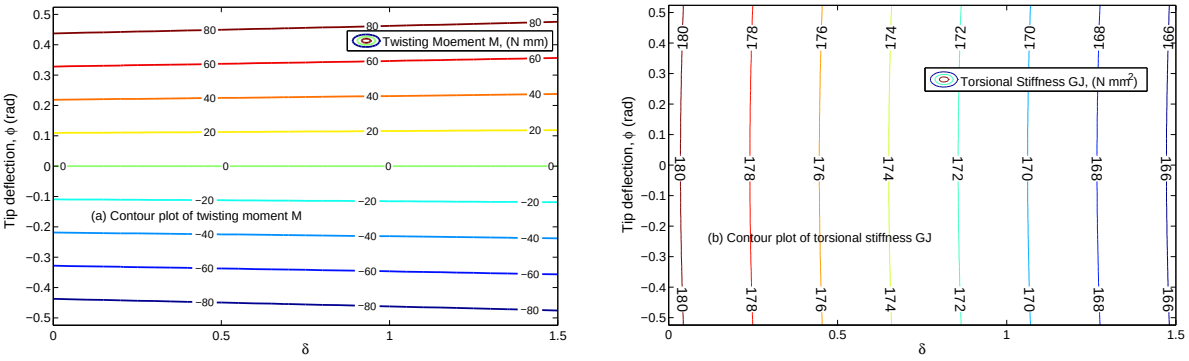

Figure 8. Effects of δ and twist angle ϕ for spar strips with a ply angle of $\beta = 90°$ on: (a) twisting moment M and (b) torsional stiffness GJ.

B. Initial curvature

In this section, three ply angles β of 0°, 45° and 90° are selected to investigate effects of initial curvatures in the middle and tip spar strips on the twist moment, torsional stiffness and stability of the SMTE.

As shown in Figs. 6 to 8, effects of δ on twist moment and torsional stiffness change significantly as the ply angle increases from 0° to 90°. For a ply angle of $\beta = 0°$, the twist moment for a certain twist angle ϕ decreases to zero while δ increases from 0 to 1.3. The torsional stiffness also reduces from 180 Nmm^2 for $\delta = 0$ to zero for $\delta = 1.3$ and

increases again to 20 Nmm^2 for $\delta = 1.5$. The ZTS SMTE case is also observed in Fig. 6 and marked by the dotted line in the plots. For a ply angle β of 45°, the increased initial curvature leads to a stable equilibrium position at positive twist angles shown by the red line marking zero twisting moment in Fig. 7a. As shown in Fig. 3 to Fig. 5, symmetric equilibria configurations of negative twist angles can be obtained as well for a ply angle of $\beta = -45°$. The torsional stiffness is not significantly affected by increasing values of δ. For a ply angle of $\beta = 90°$, the effect of varying δ on the twist moment is minor while the torsional stiffness decreases as δ increases from 0 to 1.5. Similar to a ply angle of 0°, for a given δ, the torsional stiffness remains unchanged and becomes independent of twist angle ϕ. However, no ZTS SMTE design case is found for ply angles of $\beta = 45°$ and 90°.

It is shown that changes to material stiffness and initial curvature in the prestressed spar strips significantly affect the landscapes of structural elastic strain energy, torsional stiffness as well as the stable equilibria configuration. The neutral stable position of the SMTE can be pre-defined by carefully selecting the spar strip ply angle β and the initial curvature in the prestrssed strips. This functionality provides a new design freedom of control over the SMTE concept and particularly, a ZTS SMTE is also obtained which leads to significant reduction of actuation force requirements.

IV. A zero torsional stiffness morphing trailing edge

A. Finite element method

The ZTS SMTE design found in Section III was modelled using the commercial software package ABAQUS/CAE (ABAQUS 6.12, Dassault Systems Inc., VV, France), which has a layup of $[0_8]$ for all the spar strips with 0° along the spanwise direction and a layup of $[0_4]$ for all ribs with with 0° along the chordwise direction. All the spars and ribs were modelled with S4R shell elements and after a mesh convergence analysis, a mesh seed size of approximate 4 *mm* was chosen for the model. The 8552/IM7 CFRP mechanical properties in Table. 1 were used and the laminates were modelled with Composite Layups section in Abaqus. One spanwise end of the rear spar was clamped as boundary conditions while the twist deformation was applied as a displacement boundary condition at the centroid of the other end where the reaction twist moment was measured.

With the analytical model, it is found that an initial manufactured radius of curvature $\rho = 115.1$ *mm* (corresponding to $\delta = 1.3$) in the prestressed middle and tip spar strips (see Fig. 1) leads to the ZTS of the SMTE. There are several ways to model prestress effects in the spars for instance the two-step analysis procedure used by Lachanel *et al.* [18,25] and the effective coefficients of thermal expansion (CTE) method by Daynes *et al.* [19] which requires only one model and reduces the modelling complexity. In this study, the latter method using an effective CTE is chosen and an equivalent gradient temperature field across the laminate thickness is modified to model the prestress strain caused by flattening the initial pre-bend laminates. It is shown that for a plate, a constant temperature gradient $^{\partial T}/_{\partial z}$ through the thickness causes a uniform 'spherical' curvature κ_T expressed as [26]:

$$\kappa_T = -\frac{\partial^2 w}{\partial x^2} = \alpha_x \frac{\partial T}{\partial z}, \tag{6}$$

where α_{11} denotes the CTE along x axis. With Eq.6, the bending strains caused by flattening a laminate with an initial curvature of $\triangle\kappa_x$ can be expressed as:

$$\kappa_{x,initial} = \alpha_x \frac{\partial T}{\partial z} = \frac{1}{\rho}. \tag{7}$$

Figure. 9 shows that the developed analytical model provides accurate predictions of twist moment for the SMTE compared to FEM. It is noticed that for the ZTS design, discrepancy between analytical results and FEM increases for larger twist angles. However, a significant reduction in torsional stiffness and twist moment is still observed for $\delta = 1.3$ in both the analytical model and FEM results. A parametric study using FEM shows that a further increased $\delta = 1.62$ provides a ZTS performance in FEM, as presented by the dashed black line in the plot. The difference is believed to be due to the simplicity of the analytical model used to capture the restrained warping, as the aerofoil thickness varies along the chord and in the analytical model only an averaged spar strip thickness is used to model warping restraint effects [19]. Furthermore, the stress concentration and redistribution caused by the prestress at the corners between spar strips and ribs are not modelled in the analytical model, which leads to discrepancies as well.

Interestingly, it is observed that the spanwise trailing edge deformation shape of the proposed SMTE features a typical shear/torsion deformed shape along the span as shown in Fig. 10 with a constant slope of $^{\phi}/_{L}$. A nominally deformed shape of a spanwise flap transition device by Woods *et al.* [17], is plotted against the profile obtained with the SMTE developed in this paper. Significant spanwise trailing edge deformation difference is observed and such spanwise geometrical changes significantly affect the aerodynamic and aeroacoustic performance of the wing fitted

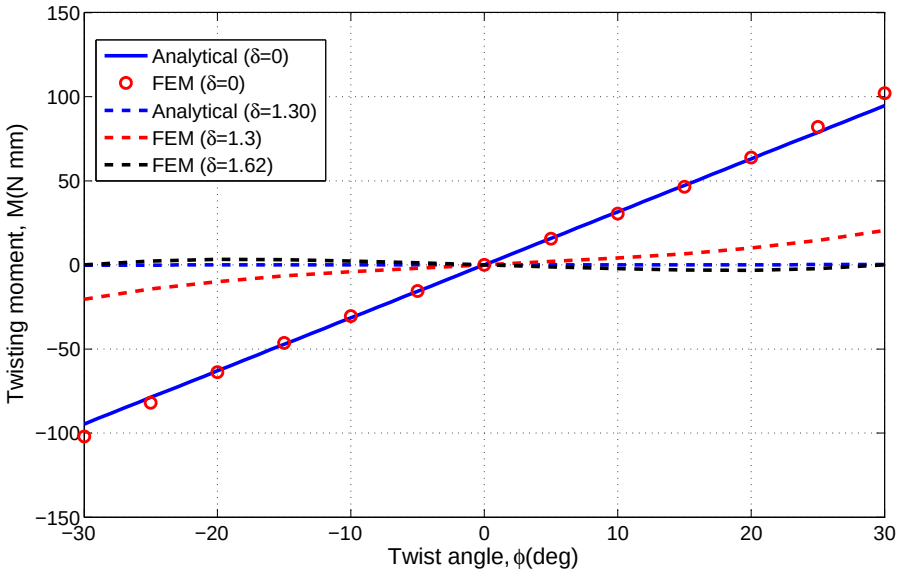

Figure 9. Verification of the analytical model–plot of twist moment M as function of twist angle ϕ

with the proposed devices. It is envisaged that further optimization studies on the spanwise trailing edge deformed shapes have great potential for improved aerodynamic and aeroacoustic performance of wings.

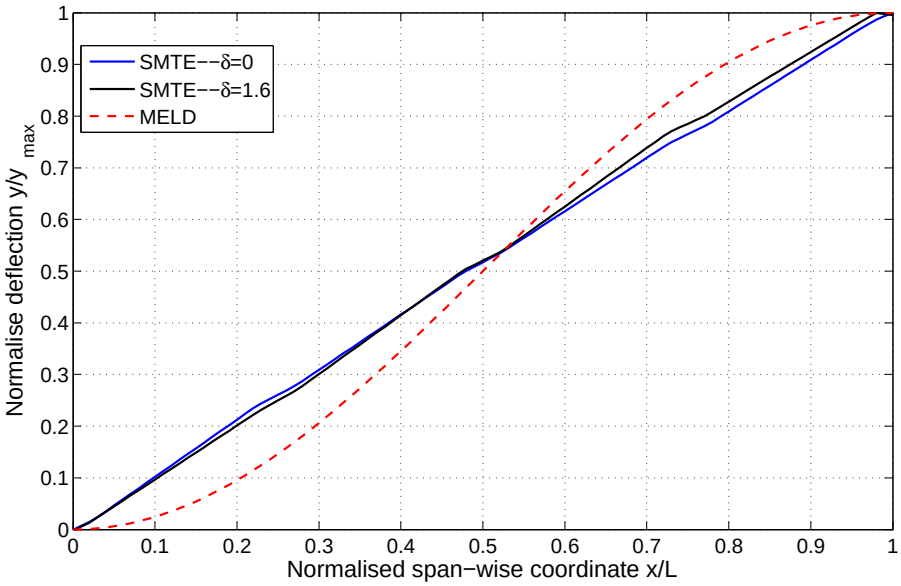

Figure 10. Spanwise trailing edge deflection of the SMTE and MELD by Woods *et al.* [17]ϕ

B. Morphing skins

In order to comprehensively investigate effects of the prestressed composite laminate spars on the stability of the SMTE, morphing skins were not considered in previous sections. Ideally, skin materials must meet a series of requirements for a viable, realistic morphing structure: [27]

- flexibility in the morphing direction to reduce actuation force;
- stiff in the non-morphing direction for structural integrity;

- high strain capability and recovery rate;
- resistance to fatigue, weather, abrasion and chemical.

Flexible matrix composites are one of the promising candidates studied [27, 28] that suit the developed SMTE design. Falken *et al.* [28] designed a novel flexible morphing skin material, the "ePreg", an elastomeric prepreg combining the high tensile strength of the carbon fibre and the high ductility of the elastomer matrix materials. Thorough studies have been carried out to assess the mechanical properties and processability and results showed that the proposed "ePreg" suits application in morphing structures. Meanwhile, functional morphing skins including the "warping skin" used by Lachenal *et al.* [18] not only provide a smooth surface and increased stiffness to resist aerodynamic loads, but also enable ease of actuation. Increased stiffness of the morphing skin does not change effects of pre-stressed spars on the SMTE and materials selection of the skin also broadens the tailorability of the whole structure.

V. Conclusions

A novel spanwise twist morphing trailing edge device consisting of CFRP ribs and spars has been proposed in this paper and preliminary optimization studies were carried out. In the developed SMTE concept, the middle and tip spar strips are prestressed by flattening a manufactured initial curvature before the structure is assembled. In this way, the SMTE grid structure is manufactured into a heightened strain energy state and yields different stable equilibrium configurations depending on the laminate layups, prestress and geometric parameters. Investigations using an analytical model are carried out and thorough parametric studies show that by selectively changing the spar laminate layups and the initial curvature in the prestressed spar strips, stable neutral position of the SMTE can be pre-defined over a wide range of twist angles (a twist angle change of $\pm 30^\circ$ has been achieved in the current design).

In particular, a zero torsional stiffness design is found for spar strips with layup of $[0_8]$ and $\delta = 1.3$ corresponding to an initial radius of curvature of 115.5 *mm* in the pre-stressed spars. The analytical model is verified using commercial FEM and good correlation was found. With the ZTS SMTE, the torsional stiffness is significantly reduced and hence the required actuation force is decreased greatly, even to zero. Though some relative minor discrepancy is observed between the proposed analytical model and FEM yet, the current model can be used for preliminary optimization studies.

Morphing skin options are briefly discussed in this paper with emphases on elastomeric matrix composites. It is believed that functional skin materials could lead to an enhanced design envelope for the proposed SMTE concept. Future work could include:

- experimental studies on the ZTS SMTE design to further investigate the mechanical properties and benchmark the developed analytical model;
- investigations on possible morphing skins and further development of the analytical model to consider skin properties;
- wind tunnel testing on the wing fitted with the developed SMTE device and/or numerical simulations to characterize effects on spanwise morphing profiles on wing performance;
- development of integrated design methods considering both spanwise and camber morphing capabilities for performance enhancement.

Acknowledgments

This work was supported by the Engineering and Physical Sciences Research Council through the EPSRC Centre for Doctoral Training in Advanced Composites for Innovation and Science [grant number EP/G036772/1]. QA would like to acknowledge the China Scholarship Council for support. Assistance from Dr. Stephen Daynes with the FEM is much appreciated.

References

[1] Advisory Council for Aviation Research ans Innovation in Europe, *Strategic Research and Innovation Agenda Executive Summary*. online, http://www.acare4europe.com/sria/exec-summary/volume-1, [Last seen on May 08, 2015].

[2] Campanile L.F. *Adaptive Structures: Engineering Applications* (Wagg D, Bond IP, Weaver PM, Friswell MI, eds). Wiley:Chichester, 2007. Chapter 4: Lightweight Shape-adaptable Airfoils: A New Challenge for an Old Dream.

[3] Lachenal X., Daynes S., Weaver P. Review of Morphing Concepts and Materials for Wind Turbine Blade Applications. *Wind Energy*, Vol.16, pp:283-307, March 2013. DOI: 10.1002/we.531.

[4] Daynes S., Weaver P.M. Review of Shape-morphing Automobile Structures: Concepts and Outlooks. *Proceedings of the Institution of Mechanical Engineers, Part D: Journal of Automobile Engineering* , Vol. 227, No. 11, pp:1603-1622, November 2013. DOI: 10.1177/0954407013496557.

[5] Dobrzynski W. Almost 40 Years of Airframe Noise Research: What did We Achieve?. *Journal of Aircraft*, 2010, Vol. 47(20), pp:353-367. Doi: 10.2514/1.44457.

[6] Weisshaar T. Morphing Aircraft Systems: Historical Perspectives and Future Challenges. *Journal of Aircraft*, Vol.50, NO. 2, pp:337- 353, March 2013. DOI: 10.2514/1.C031456.

[7] Barbarino S., Bilgen O., Aja R.M., Frishwell M.I., Inman D.J. A Review of Morphing Aircraft. *Journal of Intelligent Material Systems and Structures*, Vol. 22, NO. 9, pp:823-877, June 2011. DOI: 10.1177/1045389X11414084.

[8] Chopra I. Review of State of Art of Smart Structures and Integrated Systems. *AIAA Journal*,Vol. 40, pp:2145-2187, November 2002. DOI: 10.2514/2.1561.

[9] Campanile L.F., Anders S. Aerodynamic and Aeroelastic Amplification in Adaptive Belt-rib Airfoils. *Aerospace Science and Technology*, Vol. 9, pp:55-63, September 2004. doi:10.1016/j.ast.2004.07.007.

[10] Panesar A.S., Weaver P.M. 2012. Optimization of Blended Bistable Laminates for a Morphing Flap, *Composite Structures*, Vol. 94, No. 10, pp:3092-3105, doi:10.1016/j.compstruct.2012.05.007.

[11] Ai Q., Azarpeyvand M., Lachenal X., Weaver P. Aerodynamic and Aeroacoustic Performance of Airfoils Using Morphing Structures. *Wind Energy*, First published online: 16 September 2015, DOI: 10.1002/we.1900.

[12] Ai Q., Weaver P., Azarpeyvand M. 2016a. Design Optimization of a Morphing Flap Device Using Variable Stiffness Materials. *24th AIAA/AHS Adaptive Structures Conference, AIAA SciTech*, AIAA 2016-0816, San Diego, California, USA. DOI: 10.2514/6.2016-0816.

[13] Ai Q., Kamliya Jawahr H., Azarpeyvand M. 2016b. Experimental Investigation of Aerodynamic Performance of Airfoils Fitted with Morphing Trailing Edges. *54th AIAA Aerospace Sciences Meeting, AIAA SciTech*,AIAA 2016-1563, San Diego, California, USA.DOI: 10.2514/6.2016-1563.

[14] Kunz R. Apparatus for Closing an Air Gap between a Flap and an Aircraft, US Patent No. US4471925A. Issued Sep 18, 1984.

[15] Diller J.B., Miller N.F. Elastomeric Transition for Aircraft Control Surfaces. US Patent No. US6145791A. Issued Nov 14, 2000.

[16] Etling K.A. Morphing Control Surface Transition. US Patent No. US8342447B2, Issued Jan 1, 2013.

[17] Woods B., Parsons L., Coles A.B., Fincham J.H.S., Friswell M.I. Morphing Elastically Lofted Transition for Active Control Surfaces. *ICAST 2015: 26th International Conference on Adaptive Structures and Technologies*, October 14-16th, 2015, Kobe, Japan.

[18] Lachenal X., Daynes S., Weaver P.M. A Zero Torsional Stiffness Twist Morphing Blade as a Wind Turbine Load Alleviation Device. *Smart Materials and Structures*,Vol. 22, 065016(13pp), 2013.

[19] Daynes S., Lachenal X., Weaver P.M. Concept for Morphing Airfoil with Zero Torsional Stiffness. *Thin-walled Structures*,Vol. 94, pp. 129-134, 2015.

[20] Daynes S., Weaver P. Stiffness Tailoring Using Prestress in Adaptive Composite Structures. *Composite Structures*, 2013. Vol. 106, pp:282-287. DOI:10.1016/j.compstruct.2013.05.059.

[21] Daynes S., Weaver P.M. Analysis of Unsymmetric CFRP-Metal hybrid laminates for Use in Adaptive Structures. *Composites Part A- Applied Science and Manufacturing*, Vol. 41, pp. 1712-1718, 2010.

[22] Lachenal X., Weaver P.M., Daynes S. Influence of Transverse Curvature on the Stability of Pre-stressed Helical Structures. *International Journal of Solids and Structures*,Vol.51, 2479-2490, 2014.

[23] Kollar L.P. Springer, G.S. *Mechanics of Composite structures*. Cambridge, Uk, Cambridge University Press, 2003.

[24] Jones RM. *Mechanics of Composite Materials*. 2nd edn; Taylor and Francis:Philadelphia, 1999.

[25] Lachenal X., Weaver P.M., Daynes S. Multi-stable Composite Twisting Structure fro Morphing Applications. *Proceedings of the Roal Society A-Mathematical, Physical and Engineering Sciences*,Vol.468,1230-1251, 2012.

[26] Mansfield E.H. *The Bending and Stretching of Plates*. Cambridge, UK, Cambridge University Press, 22 Aug 2005.

[27] Thill C., Etches J., Bond I., Potter K., Weaver P. Morphing skins. *The Aeronautical Journal*, Vol. 112, pp:117-139.

[28] Falken A., Steeger S., Heintze O. From Development of Multi-material Skins to Morphing Flight Hardware Production. *24th AIAA/AHS Adaptive Structures Conference*, AIAA SciTech, 4th-8th Jan, 2016, San Diego, California, USA.